Astronomy & Astrophysics manuscript no. Ec_flat_2020July06
July 6, 2020

The cyclotron line energy in Her X-1: stable after the decay

R. Staubert[1], L. Ducci[1], L. Ji[1], F. Fürst[2], J. Wilms[3], R.E. Rothschild[4], K. Pottschmidt[5], M. Brumback[6], F. Harrison[7]

[1] Institut für Astronomie und Astrophysik, Universität Tübingen, Sand 1, 72076 Tübingen, Germany
[2] European Space Agency - European Space Astronomy Center (ESA-ESAC), Operations Dpt., Camino Bajo del Castillo, s/n., Urb. Villafranca del Castillo, 28692 Villanueva de la Canada, Madrid, Spain
[3] Dr. Remeis Sternwarte & Erlangen Centre for Astroparticle Physics, Univ. Erlangen-Nürnberg, Sternwartstr. 7, 96049 Bamberg, Germany
[4] Center for Astrophysics and Space Sciences, University of California at San Diego, La Jolla, CA 92093-0424, USA
[5] NASA-Goddard Spaceflight Center, 8800 Greenbelt Rd., Greenbelt, MD 20771, USA
[6] Dartmouth College, Department of Physics & Astronomy, 6127 Wilder Laboratory, Hannover, NH 03755, USA
[7] Cahill Center for Astronomy and Astrophysics, California Institute of Technology, Pasadena, CA 91125, USA

submitted: 06/07/2020, accepted: ****

ABSTRACT

We summarize the results of a dedicated effort between 2012 and 2019 to follow the evolution of the cyclotron line in Her X-1 through repeated *NuSTAR* observations. The previously observed nearly 20-year long decay of the cyclotron line energy has ended around 2012: from there onward the pulse phase averaged flux corrected cyclotron line energy has remained stable and constant at an average value of $E_{\rm cyc} = (37.44 \pm 0.07)$ keV (normalized to a flux level of 6.8 *RXTE*/ASM-cts/s). The flux dependence of $E_{\rm cyc}$ discovered in 2007 is now measured with high precision, yielding a slope of (0.675 ± 0.075) keV/(ASM-cts/s), corresponding to an increase of 6.5% of $E_{\rm cyc}$ for an increase in flux by a factor of two. We also find that all line parameters as well as the continuum parameters show a correlation with X-ray flux. While a correlation between $E_{\rm cyc}$ and X-ray flux (both positive and negative) is now known for several accreting binaries with various suggestions for the underlying physics, the phenomenon of a long-term decay has so far only been seen in Her X-1 and Vela X-1, with far less convincing explanations.

Key words. magnetic fields, neutron stars, – radiation mechanisms, cyclotron scattering features – accretion, accretion columns – binaries: eclipsing – stars: Her X-1 – X-rays: general – X-rays: stars

1. Introduction

The X-ray spectrum of the accreting binary pulsar Her X-1 is characterized by a power law continuum with exponential cut-off and an apparent line-like feature, which was discovered in 1975 (Trümper et al. 1978). This feature is now generally accepted as an absorption-like feature around 40 keV due to resonant scattering of photons off electrons on quantized energy levels (Landau levels) in the teragauss magnetic field at the polar cap of the neutron star. The feature is therefore often referred to as a cyclotron resonant scattering feature (CRSF). The energy spacing between the Landau levels is given by $E_{\rm cyc} = \hbar eB/m_{\rm e}c = 11.6\,{\rm keV}\,B_{12}$, where B_{12} is the strength of the magnetic field in units of 10^{12} Gauss, providing a direct method of measuring the magnetic field strength at the site of the emission of the X-ray spectrum. The observed line energy is subject to gravitational redshift, z, such that the magnetic field may be estimated by $B_{12} = (1+z)E_{\rm obs}/11.6\,{\rm keV}$ (Schwarm et al. 2017). The discovery of the cyclotron feature in the spectrum of Her X-1 provided the first ever direct measurement of the magnetic field strength of a neutron star, in the sense that no other model assumptions are needed. Originally considered an exception, cyclotron features are now known to be rather common in accreting X-ray pulsars; about 35 binary pulsars are now known to be cyclotron line sources. In several objects, multiple lines (up to four harmonics) have been detected (for reviews, see Staubert et al. 2019; Revnivtsev & Mereghetti 2016; Caballero & Wilms 2012; Wilms 2012; Terada et al. 2007; Heindl et al. 2004; Staubert 2003; Coburn et al. 2002).

The Her X-1/HZ Her binary system shows strong variability on very different timescales: the 1.24 s spin period of the neutron star, the 1.7 d binary period, the 35 d flux modulation, and the 1.65 d period of the pre-eclipse dips (Tananbaum et al. 1972). The 35 d *On-Off* variation can be understood as being due to the precession of a warped accretion disk (Petterson 1977; Schandl & Meyer 1994). Due to the high inclination of the binary ($i > 80°$) we see the disk nearly edge-on. The precessing warped disk therefore covers the central X-ray source during a substantial portion of the 35 d period. Furthermore, a hot X-ray heated accretion disk corona reduces the X-ray signal (energy independently) by Compton scattering whenever it intercepts our line of sight to the neutron star. As a result, the X-ray source is covered twice during a 35 d cycle. A further modulation appears through the so-called *Anomalous Lows* (ALs) that reduce the X-ray flux to very low levels for time periods ranging from days to years (see, e.g., five ALs observed between 1984 and 2015 listed by Staubert et al. 2017). ALs are probably caused by a low inclination of the accretion disk, possibly combined with a thickening of the inner part of the accretion disk, thereby shading the X-ray emitting regions at the poles of the neutron star. The ALs tend to appear on a quasi-period of ∼5.5 yr if we assume that two out of seven ALs were actually not realized (at least not observed).

The centroid energy $E_{\rm cyc}$ of the CRSF in Her X-1 is variable with respect to several parameters, namely pulse phase, luminosity, time, and possibly a 35 d phase (Staubert et al. 2014). Apart

Send offprint requests to: staubert@astro.uni-tuebingen.de

Table 1. Details on *NuSTAR* observations of Her X-1 between 2012 and 2020.

Observation date	Obs ID	35-day cycle no.[a]	Start of obs [MJD]	End of obs [MJD]	Center of obs [MJD]	Net exposure [ksec]	35-day *Turn-On*[b] [MJD]	35-day phase[c] of center of obs
22 Sep 2012	30002006005[d]	427	56192.19	56192.77	56192.48	~22	56189.0 ± 0.1	0.100
03 Aug 2015	90102002002	457	57237.69	57238.26	57237.98	22.5	57233.5 ± 0.1	0.128
20 Aug 2016	10202002002	468	57620.19	57621.26	57620.73	36.6	57617.2 ± 0.1	0.101
05 Aug 2017	30302012002	478	57970.42	57971.21	57970.81	28.4	57965.7 ± 0.2	0.147
26 Feb 2018	30302012004	484	58175.07	58175.79	58175.43	18.3	58171.5 ± 0.5	0.113
17 Sep 2018	30402009002	490	58378.83	58379.56	58379.19	28.4	58377.7 ± 0.3	0.044
09 Feb 2019	30402034002	494	58523.41	58523.85	58523.63	18.3	58516.6 ± 0.2	0.202[e]
14 Mar 2019	30402034008	495	58556.28	58556.75	58556.51	4.3	58551.5 ± 0.7	0.144
23 Jun 2019	30402009004	498	58657.34	58658.06	58657.70	27.1	58654.1 ± 0.2	0.102

[a] 35-day cycle numbering is according to Staubert et al. (1983); [b] as determined from the monitoring data of *Swift*/BAT; [c] using $P_{35} = 34.85$ d; [d] see Fürst et al. (2013), Table 1; [e] this observation is at a particular high 35-day phase.

Table 2. Summary of the spectral analysis of nine *NuSTAR* observations of Her X-1. The spectral parameters were found by applying the XSPEC-function `highecut` (see text). Uncertainties are at the 1 sigma (68%) level. The maximum flux of the respective 35-day cycle is given in units of (ASM-cts/s), referring to the All Sky Monitor of *RXTE*. The corresponding physical flux in units of (keV/cm^2 s) results by multiplying with 0.236. The flux was actually measured by *Swift*/BAT and converted according to (2–10 keV) (ASM − cts/s) = 93.0 × (15–50 keV) (BAT − cts/cm^2 s) (Staubert et al. 2016). The observed line energy was normalized to an ASM-count rate of 6.8 cts/s by using a slope of (0.675 ± 0.075) keV/(ASM-cts/s) (see Fig. 1).

35 d cycle no.[e]	max. flux of 35 d cycle [ASM-cts/s]	Observed line energy [keV]	Line width σ [keV]	Line strength[a] [keV]	$E_{\rm cyc}$ norm. to 6.8 ASM-cts/s [keV]	$E_{\rm cut}$ [keV]	$E_{\rm fold}$ [keV]	Power law index Γ
427	6.60 ± 0.20	37.40 ± 0.25[b]	5.76 ± 0.29	8.86 ± 0.87	37.54 ± 0.25	20.68 ± 0.27	9.95 ± 0.13	0.920 ± 0, 004
457	2.96 ± 0.28	34.79 ± 0.22	4.46 ± 0.22	4.70 ± 0.70	37.38 ± 0.24[c]	19.86 ± 0.12	9.37 ± 0.09	0.929 ± 0.003
468	6.50 ± 0.20	37.18 ± 0.14	5.97 ± 0.18	8.83 ± 0.44	37.38 ± 0.14[c]	20.86 ± 0.15	10.16 ± 0.07	0.985 ± 0.001
478	4.10 ± 0.15	35.62 ± 0.18	4.94 ± 0.20	5.90 ± 0.40	37.44 ± 0.19	19.98 ± 0.16	9.79 ± 0.09	0.962 ± 0.002
484	4.09 ± 0.19	35.67 ± 0.29	4.84 ± 0.33	6.10 ± 0.70	37.50 ± 0.30	20.04 ± 0.11	10.16 ± 0.07	0.963 ± 0.002
490	5.60 ± 0.22	36.65 ± 0.16	5.61 ± 0.25	8.44 ± 0.59	37.46 ± 0.16	20.45 ± 0.23	9.79 ± 0.09	0.974 ± 0.002
494	5.02 ± 0.20	36.28 ± 0.22	5.26 ± 0.24	7.21 ± 0.53	37.48 ± 0.23	19.56 ± 0.12	9.65 ± 0.11	0.885 ± 0.002[f]
495	3.72 ± 0.56	35.36 ± 0.41	4.76 ± 0.45	6.38 ± 0.98	37.44 ± 0.43	19.62 ± 0.29	9.49 ± 0.24	0.934 ± 0.005
498[d]	4.00 ± 0.37	35.65 ± 0.21	5.01 ± 0.25	7.02 ± 0.50	37.54 ± 0.22	19.81 ± 0.16	9.38 ± 0.09	0.932 ± 0.001

[a] note that strength = $\sigma\ \tau\ \sqrt{2\pi}$;
[b] the values for the CRSF are from Fürst et al. (2013), Obs. II (Table 3, HighE);
[c] in Staubert et al. (2016, 2017) the flux normalization was done with a slope of 0.44 (instead of 0.675);
[d] for the June 2019 observation only data from detector B have been used (see text);
[e] 35-day cycle numbering is according to Staubert et al. (1983);
[f] observation at a high 35-day phase, Γ expected to be lower (Vasco 2012).

from the discovery of the first CRSF ever, Her X-1 (through repeated observations) has allowed the first discovery of two additional features with respect to its CRSF, both of which have in the meantime been observed in other binary X-ray pulsars. First, a positive correlation between $E_{\rm cyc}$ and the X-ray luminosity L_x (Staubert et al. 2007) (confirmed on short timescales by the pulse-amplitude-resolved technique by Klochkov et al. 2011), and second, a long-term decay of $E_{\rm cyc}$, co-existing with the luminosity dependence (Staubert et al. 2014, 2016). The long-term decay was confirmed by Klochkov et al. (2015) using monitoring data of *Swift*/BAT (even without taking the luminosity dependence into account).

In addition to Her X-1 there are now six other sources known that show such a positive correlation between the line energy and the X-ray luminosity (see the summary in Staubert et al. 2019). At very high luminosity only one source exists - V 0332+53 - with a well secured negative correlation (Staubert et al. 2019). With regard to the long-term decay in $E_{\rm cyc}$, there are now two clear cases: Her X-1 and Vela X-1). For Vela X-1 the effect is only seen in the first harmonic at ~53 keV (La Parola et al. 2016; Ji et al. 2019). Two further candidates with a somewhat strange behavior are V0332+53 during an outburst (Cusumano et al. 2016; Doroshenko et al. 2017; Vybornov et al. 2018), and 4U 1538−522 (Hemphill et al. 2016) (on longer time scales).

Here we summarize the results of nine observations of Her X-1 by *NuSTAR* in the time frame 2012 to 2019 with regard to the cyclotron resonance scattering feature in the pulse averaged X-ray spectrum: the CRSF energy has apparently stopped

its ~20 -year long decay and has stayed constant since around 2012. In addition to the CRSF centroid energy also its width and strength are clearly correlated with flux, the dependencies are now measured with high precision.

2. Observations and analysis

In Table 1 we list nine observations of Her X-1 performed by *NuSTAR* (Harrison et al. 2013) over the time period 2012 to 2019, all done close to the maximum flux of a *Main-On* state. Also given are the net exposure times (varying between 4.3 ks and 36.6 ks), the times of the respective 35-day *Turn-On* and the 35-day phase of the center of the respective observations. The details of the data analysis are similar to those described by Staubert et al. (2014) and Staubert et al. (2016). We used the standard `nupipeline` and `nuproducts` utilities (01Apr20_v1.9.2) and XSPEC[1] v12.11 as part of HEASOFT[2]. The source extraction diameter was selected between 90 arcsec and 120 arcsec depending on the brightness of the source. All values given are from simultaneous spectral fitting of the data from both focal plane detectors, unless otherwise stated. The spectral function used for all observations was the XSPEC-function `highecut` in combination with a `power law`:

$$I_E = \begin{cases} K \cdot E^{-\Gamma}, & \text{if } E \le E_{\rm cut} \\ K \cdot E^{-\Gamma} \exp\left(-\frac{E-E_{\rm cut}}{E_{\rm fold}}\right), & \text{if } E > E_{\rm cut}. \end{cases} \quad (1)$$

where Γ is the power law (photon) index, $E_{\rm cut}$ is the energy where the cut-off sets in, and $E_{\rm fold}$ is the e-folding energy describing the flux decay. The function contains a discontinuity of its first derivative (a "break") at $E = E_{\rm cut}$. In order to smooth this break, generally an artificial small Gaussian absorption line was added with the center energy fixed to $E_{\rm cut}$ and a free width and depth. Neither the power law, nor the exponential cut off are affected by this (e.g., Coburn et al. 2002).

The cyclotron line is modeled by the Gaussian shaped "`gabs`" function: To model the cyclotron line, one modifies the continuum functions described above by the inclusion of a corresponding multiplicative component of the form $e^{-\tau(E)}$, where the optical depth $\tau(E)$ has a Gaussian profile:

$$\tau(E) = \tau_0 \exp\left[-\frac{(E - E_{\rm cyc})^2}{2\sigma_{\rm cyc}^2}\right], \quad (2)$$

with τ_0, $E_{\rm cyc}$, and $\sigma_{\rm cyc}$ being the central optical depth, the centroid energy, and the width of the line. We note that in the popular *XSPEC* realization of this function `gabs`, τ_0 is not explicitely used as a fit parameter. Instead, a product $\tau_0 \sqrt{2\pi}\sigma_{\rm cyc}$ is defined as the *"strength"* of the line.

Some of the listed *NuSTAR* observations have been performed in coordination with other satellites, like *INTEGRAL*, *Insight*-HXMT and *Astrosat* to study the CRSF. The February and March 2019 observations were coordinated with XMM-Newton for a different project[3], but also yielded data on the CRSF. Here we will not report on the results from the other satellites since we are still working on trying to resolve some inconsistencies, which are likely due to imperfect inter-calibration between the different instruments and possibly aging of some of them[4] - we plan to report about this in a forthcoming paper. See e.g., Xiao et al. 2019 for one comparison to *Insight*-HXMT. Two other publications on observations by *Astrosat* and *Insight*-HXMT are in preparation.

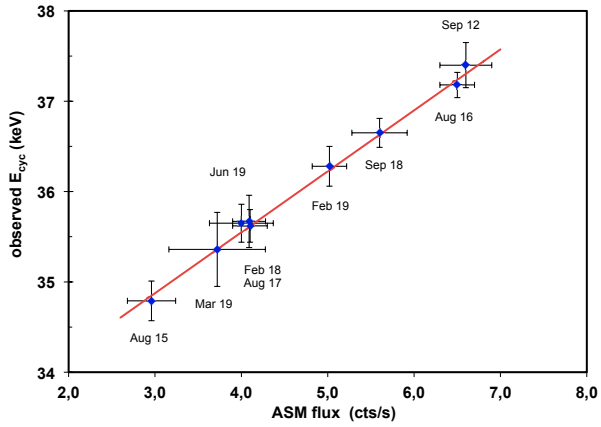

Fig. 1. Correlation between the measured values of the pulse phase averaged cyclotron line energy and the X-ray flux measured by *Swift*/BAT (in units of (ASM-cts/s)) for all *NuSTAR* observations between 2012 and March 2019 (see Table 1). Note that 1 (ASM-cts/s) equals 93.0 (Swift-BAT-cts)/(s keV) (Staubert et al. 2016) and 0.236 (keV/cm^2 s) in (2–10 keV). The best fit line defines a slope of (0.675 ± 0.075) keV/(ASM − cts/s). Pearsons linear correlation coefficient is 0.98.

3. Results

In Table 2 we summarize the results of the spectral analysis, both for the cyclotron line (the centroid energy, the width and the strength) and for the continuum (cut-off energy $E_{\rm cut}$, e-folding energy $E_{\rm fold}$ and power law index Γ). We further list the maximum fluxes of the respective 35-day cycles. In order to allow a comparison to previous results, we use the observational flux units of (ASM-cts/s), referring to the All Sky Monitor of *RXTE*), using the conversion (2–10 keV) (ASM-cts/s) = 93.0 × (15–50 keV) (BAT-cts/cm^2 s). This was found by Staubert et al. (2016) by comparing flux values measured by the All Sky Monitor onboard of *RXTE* on the one hand and those from *Swift*/BAT on the other, for the overlapping time of both missions. The physical flux units, referring to the energy range of (2-10) keV, corresponding to the ASM count rate are the following: Flux [keV/cm^2 s] = 0.236 × (ASM-cts/s), or Flux [erg/cm^2 s] = 3.78 10^{-10} × (ASM-cts/s). Also listed are the cyclotron line energies normalized to a flux of 6.8 (ASM-cts/s) using the determined linear flux dependence (Fig. 1): $E_{\rm cyc-norm}$ [keV] = $E_{\rm cyc-obs}$ [keV] + 0.675 × ((ASM-cts/s)-6.8). Pearsons linear correlation coefficient is 0.98.[5]

Generally, all parameter values stated are from the combined spectral analysis of both focal plane detectors of *NuSTAR*, except for the observation in June 2019 (cycle 498): only focal plane detector B was used, for $E_{\rm cut}$ the value from detector A is

[1] https://heasarc.gsfc.nasa.gov/xanadu/xspec/
[2] http://heasarc.nasa.gov/lheasoft, 6.27.2, caldb release 20191219.
[3] Brumback et al. 2020, in preparation
[4] We are still attempting to perform further simultaneous observations between *NuSTAR*, *INTEGRAL* and *Insight*-HXMT, some are already planned.
[5] see e.g., Numerical Recipes, W.H. Press et al., Cambridge University Press, 1986

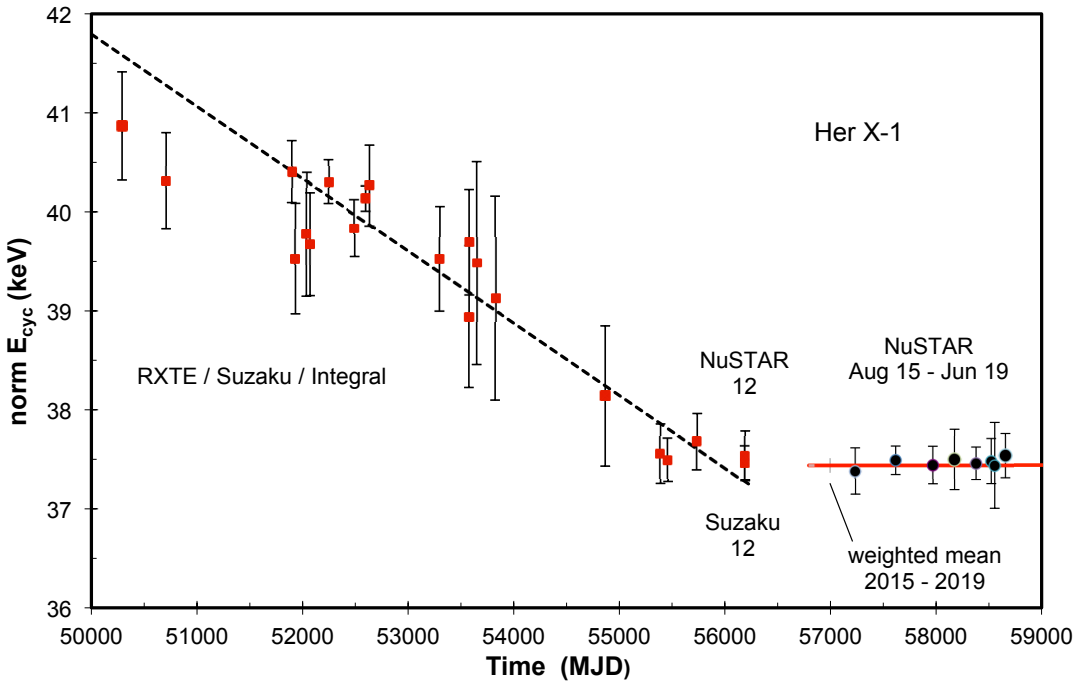

Fig. 2. Evolution of the cyclotron line energy $E_{\rm cyc}$ in Her X-1. The red points until 2012 (MJD 56200) and the corresponding linear best fit (dashed line) are reproduced from Staubert et al. (2016). The black points are the new measurements by *NuSTAR* from 2015-2019 (see Table 1): the pulse phase averaged $E_{\rm cyc}$ values normalized to a reference ASM count rate of 6.8 (ASM − cts/s) using a flux dependence of 0.675 keV/(ASM − cts/s) (see Fig. 1). The solid red line represents the weighted mean of (37.44 ± 0.07) keV, demonstrating a constant value since at least 2012.

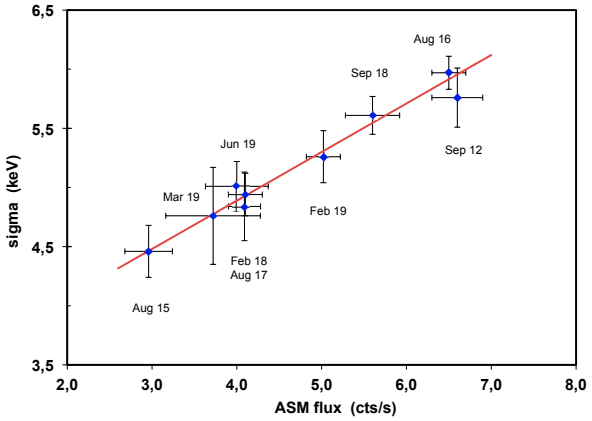

Fig. 3. Correlation between the measured values of the width (sigma) of the cyclotron line and the X-ray flux. The fit takes into account nine measurements by *NuSTAR* from 2012-2019 (see Table 1). The best fit line is given by the function $sig_{\rm cyc}$ = (5.30 ± 0.09) + (0.41 ± 0.07) × ((ASM − cts/s) − 5.0) (all values in keV). Pearsons linear correlation coefficient is 0.99.

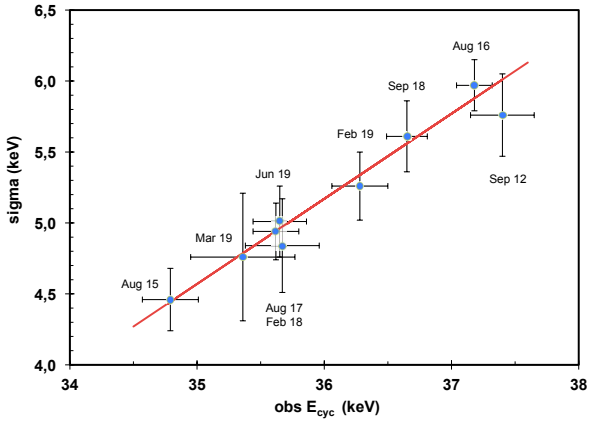

Fig. 4. Correlation between the width (sigma) of the pulse phase averaged cyclotron line and its centroid energy. The fit takes into account nine measurements by *NuSTAR* from 2012-2019 (see Table 1). The best fit line is given by the function $\sigma_{\rm cyc} = (5.17 \pm 0.09) + (0.60 \pm 0.11) \times (E_{\rm cyc} - 36.0)$ (all values in keV). Pearsons linear correlation coefficient is 0.96.

exceptionally high and far outside the overall trend (Fig. 7) (the anomaly is being investigated).

3.1. Cyclotron line parameters

The new data allow us to determine the correlation between the observed pulse averaged cyclotron line energy and the X-ray flux

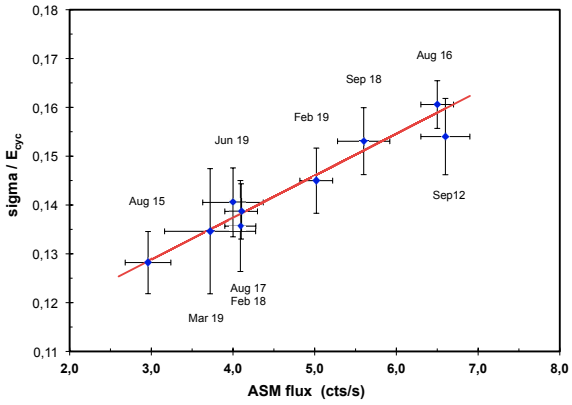

Fig. 5. The relative width of the cyclotron line versus X-ray flux in units of (ASM-cts/s). The best fit line is given by the function $\sigma_{\rm cyc}$ / $E_{\rm cyc}$ = (0.146 ± 0.002) + (0.0086 ± 0.0019) × ((*ASM* − *cts*/*s*) − 5.0). Pearsons linear correlation coefficient is 0.97.

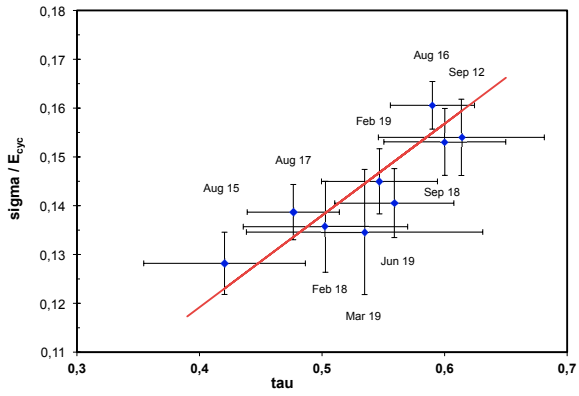

Fig. 6. The relative width of the cyclotron line versus optical depth τ. The best fit line is given by the function $\sigma_{\rm cyc}$ / $E_{\rm cyc}$ = (1.38 ± 0.005) + (0.188 ± 0.076) × ($\tau_{\rm cyc}$ − 0.5). Pearsons linear correlation coefficient is 0.88.

with a significantly improved accuracy when compared to the time of the discovery of this correlation (Staubert et al. 2007). Fig. 1 shows the definite correlation which can be described by the linear function $E_{\rm cyc}$ [keV] = $a + b \times$ ((ASM − cts)/s − 6.8), with a = (37.44 ± 0.07) being the CRSF value at an ASM count rate of 6.8 cts/s and b = (0.675 ± 0.075) keV/(ASM − cts)/s the slope describing the flux dependence.

Figure 2 displays the evolution of the normalized CRSF centroid energy of Her X-1 from 2009 to 2019. The red data points are historical results that were published before, together with the dashed line representing the end of the phase of the long-term decay of $E_{\rm cyc}$ between 1996 and 2012 as reported by Staubert et al. (2016) (their Fig. 2). The right hand side shows the latest values from *NuSTAR* (2015-2019). All data points are flux corrected (normalized to an ASM cout rate of 6.8 cts/s). The values since 2015 are apparently consistent with a constant value, the formal weighted average is $\langle E_{\rm cyc}\rangle(2015-2019)$ = (37.44 ± 0.07) keV. Since there is no time dependence, it is not necessary to perform a combined fit with simultaneously existing flux and time dependencies, as was done for the data earlier than 2012 (Staubert et al. 2016).

We need to point out, however, that the new data require a modification of the view presented in Staubert et al. (2017), in which it was suggested that an inversion (an upward trend) in $E_{\rm cyc}$ had occured after the end of the decay. This impression was mainly driven by the 2015 measurement which happened at an extremely low flux level - in fact the lowest of all *NuSTAR* observations at around 3 (ASM-cts)/s (see Fig. 1). This had, on the one hand, turned out to be useful since it extended the dynamic range in observed fluxes beyond the (classical) factor of two, it led, on the other hand, to a very low value of the flux normalized $E_{\rm cyc}$ when the correction was done with the then best value of the flux dependence of 0.44 keV/(ASM − cts/s) (Staubert et al. 2016, 2017). When the current best value (0.675 instead of 0.44) is used for the normalization, the 2015 value is significantly higher and consistent with values found throughout 2012–2019 (see Table 1 and Fig. 2).

A further result of our analysis of the nine *NuSTAR* observations is that we find that also all other characteristic parameters of the cyclotron line – the width σ, the "strength", the optical depth τ and the relative width - are linearly correlated with the X-ray flux. In Table 3 we summarize the results of linear fits of all the CRSF line parameters versus flux. This also means that all line parameters correlate to one-another linearly. As an example, Fig. 3 shows the dependence of the line width σ on flux and Fig. 4 the dependence of σ on $E_{\rm cyc}$. This correlation is a well known behavior (apparently valid for all cyclotron line sources, e.g., Makishima et al. (1999); Coburn et al. (2002)), that is expected to occur through thermal Doppler broadening because of the free movement of electrons along the magnetic field lines (see discussion below). Even though the correlations between the different parameters can in principle be re-constructed from the respective dependencies of all parameters on flux (Table 3), we have performed the linear fits for every possible pair of parameters explicitely and summarize the results in Table 4.

Table 3. The linear dependence of spectral parameters on X-ray flux. The five line parameters are the centroid energy $E_{\rm cyc}$, the width $\sigma_{\rm cyc}$, the line "strength", the optical depth τ (see eq. 2) and the relative width $\sigma_{\rm cyc}$ / $E_{\rm cyc}$. The three continuum parameters are $E_{\rm cut}$ and $E_{\rm fold}$ and the power law photon index Γ. The X-ray flux is measured in units of (ASM-cts/s), referring to the All Sky Monitor of *RXTE*): y = a + b (x - c). Here, the offset in x is always constant: c = 5.0 (ASM-cts/s) (close to the center of the range of fluxes observed). Note that 5.0 (ASM-cts/s) corresponds to 5.0× 0.236 = 1.18 (keV/cm^2 s) in (2–10 keV). Uncertainties are at the 1 sigma (68%) level. The last column lists Pearsons linear correlation coefficients.

Parameters	a [keV] or no dimension	b[d]	Pearsons corr. coeff.
$E_{\rm cyc}$[a] [keV]	36.24 ± 0.09	0.675 ± 0.075	0.98
$\sigma_{\rm cyc}$[b] [keV]	5.30 ± 0.09	0.41 ± 0.07	0.99
strength[c]	7.28 ± 0.22	1.15 ± 0.19	0.96
opt. depth τ[c]	0.54 ± 0.02	0.042 ± 0.015	0.87
$\sigma_{\rm cyc}$ / $E_{\rm cyc}$	0.146 ± 0.002	0.0086 ± 0.0002	0.97
$E_{\rm cut}$ [keV]	20.17 ± 0.06	0.30 ± 0.06	0.74
$E_{\rm fold}$ [keV]	9.83 ± 0.04	0.24 ± 0.03	0.79
Γ	0.965 ± 0.002	0.015 ± 0.001	0.53

[a] Fig. 1; [b] Fig. 3; [c] note that strength [keV] = $\sigma \times \tau \times \sqrt{2\pi}$;
[d] [keV/(ASM-cts/s)] or [1/(ASM-cts/s)]

Table 4. Relations between line parameters, $y = a + b\,(x - c)$: parameter y (top line) versus parameter x (first column). The offset c is constant for any given parameter x. Uncertainties are at the 1 sigma (68%) level.

Parameter versus	E_{cyc} [keV]	σ_{cyc} [keV]	strength [keV]	τ	σ_{cyc} / E_{cyc}
E_{cyc}	—-	$a = 5.17 \pm 0.09$	$a = 6.91 \pm 0.22$	$a = 0.53 \pm 0.02$	
	—-	$b = 0.60 \pm 0.11$	$b = 1.71 \pm 0.29$	$b = 0.064 \pm 0.023$	
	—-	$c = 36.0$ keV	$c = 36.0$ keV	$c = 36.0$ keV	
σ_{cyc}		—-	$a = 6.42 \pm 0.31$	$a = 0.51 \pm 0.02$	
		—-	$b = 2.84 \pm 0.63$	$b = 0.11 \pm 0.04$	
		—-	$c = 5.0$ keV	$c = 5.0$ keV	
strength			—-	$a = 0.53 \pm 0.02$	
			—-	$b = 0.041 \pm 0.014$	
			—-	$c = 7.0$	
τ				—-	$a = 0.14 \pm 0.05$
				—-	$b = 0.19 \pm 0.08$
				—-	$c = 0.50$
E_{cut}	$a = 35.86 \pm 0.11$				
	$b = 1.87 \pm 0.36$				
	$c = 20.0$ keV				
E_{fold}	$a = 36.69 \pm 0.13$				
	$b = 2.71 \pm 0.39$				
	$c = 10.0$ keV				

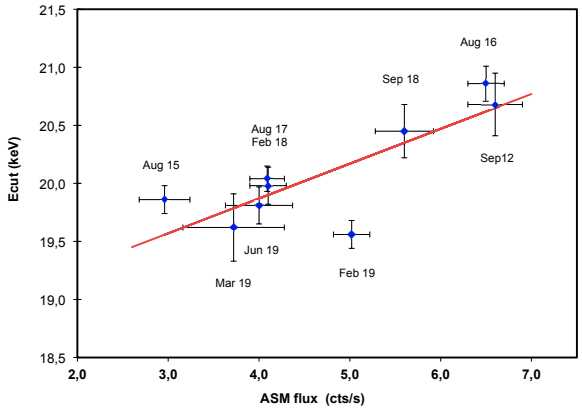

Fig. 7. The continuum parameter E_{cut} versus X-ray flux in units of (ASM-cts/s). The value for the June 2019 observation is from focal plane detector B only (see text). The best fit line is given by the function $E_{cut} = (20.17 \pm 0.06) + (0.30 \pm 0.06) \times (ASM - 5.0)$ (all values in keV). Pearsons linear correlation coefficient is 0.74.

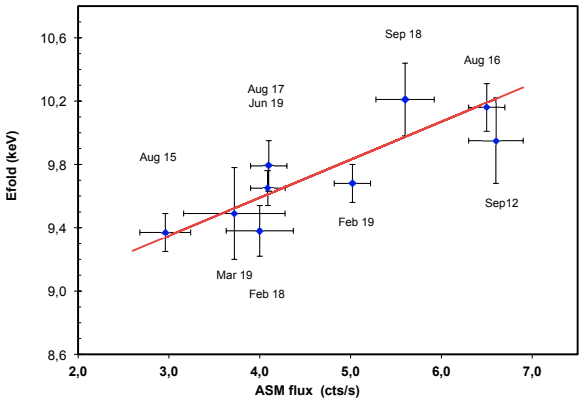

Fig. 8. The continuum parameter E_{fold} versus X-ray flux in units of (ASM-cts/s). The best fit line is given by the function $E_{fold} = (9.83 \pm 0.04) + (0.24 \pm 0.03) \times ((ASM - ct/s) - 5.0)$ (all values in keV). Pearsons linear correlation coefficient is 0.79.

It is worth to note that the relative line width, σ / E_{cyc}, is not constant, but increases with increasing flux (Fig. 5) according to σ / E_{cyc} = 0.146 + 0.0087 (ASM - 5.0). This means that the relative change with changing flux is stronger for the line width than for the line energy.

In addition, we give the linear correlation between the relative line width σ / E_{cyc} to the optical depth τ (Fig.6), a correlation first noticed by Coburn et al. (2002) in a group of cyclotron line objects. As with other correlations, also this one can be realized in individual objects - here Her X-1, also in 4U 1538−52 (Rodes-Roca et al. 2008). This may not be so easy to understand in the context of theoretical considerations (see discussion).

3.2. Continuum parameters

The systematic monitoring of Her X-1 with *NuSTAR* over the last decade has allowed the discovery that all continuum parameters, E_{cut}, E_{fold} and Γ are systematically correlated with X-ray flux. The correlations can be described by linear functions, see Table 3, Fig. 7, Fig. 8 and Fig. 9. Since both E_{cut} and E_{fold} depend on X-ray flux, they correlate with each other which is shown in Fig. 10. Normalizing E_{cut} and E_{fold} to the reference flux of 5.0 (ASM-cts/s), we find that both normalized parameters are consistent with a constant value over the time span 2012-2019 (Fig. 13). In calculating the dependence of Γ on flux we have excluded the exceptionally low value (0.885) measured in February

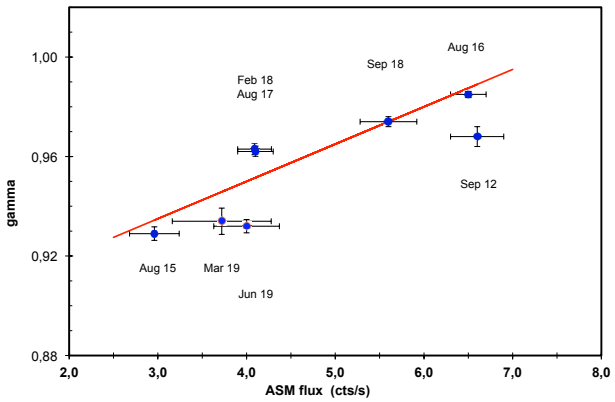

Fig. 9. The power law index Γ versus flux in (ASM-cts/s). The best fit line is given by the function Γ = (0.965 ± 0.002)+(0.015 ± 0.001) × ((ASM-cts/s) - 5.0). This function is valid for 35-day phases up to 0.16. The low Γ value measured in Feb 2019 (cycle 494, see Table 2) was not included in this fit since the observation took place at a 35-day phase of 0.202, at which a lower value is expected (see text). Pearsons linear correlation coefficient is 0.53.

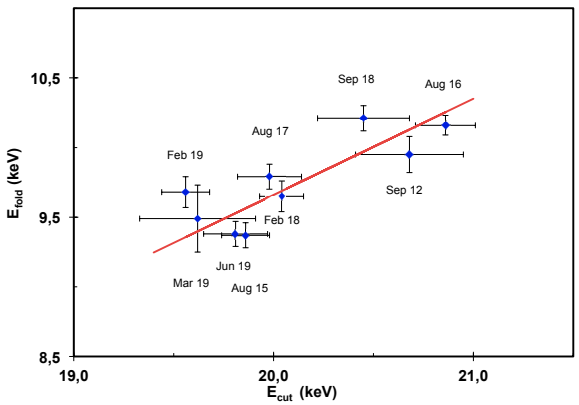

Fig. 10. The continuum parameter $E_{\rm fold}$ versus the continuum parameter $E_{\rm cut}$. The best fit line is given by the function $E_{\rm fold}$ = (9.66 ± 0.05) + (0.69±0.12)×($E_{\rm cut}$−20.0) (all values in keV). Pearsons linear correlation coefficient is 0.82.

2019 (cycle 494, see Table 2) because the observation was performed at a high 35-day phase of 0.202, where the flux is about 65% of the maximum *Main-On* flux of this cycle. At 35-day phases beyond ~0.16, Γ is known to decrease (Vasco 2012). The measured increase of Γ on flux is fairly weak but interesting because this is in disagreement with reports about a correlation in the opposite sense by Klochkov et al. (2011) (see the discussion below).

3.3. Correlation between line and continuum parameters

Since the continuum parameters $E_{\rm cut}$ and $E_{\rm fold}$ and all cyclotron line parameters correlate with X-ray flux, there are correlations between the line and the continuum parameters. As two examples we list the linear correlation parameters of the observed cyclotron line energy and the continuum parameters in Table 4 and show them in Fig. 11 and Fig. 12.

3.4. Dependence on phase of the 35-day modulation

As mentioned in the Introduction, Her X-1 shows a regular 35-day modulation, known since the discovery of the source by *UHURU* (Tananbaum et al. 1972), thought to be connected with the precession of the accretion disk providing regular shadowing of the X-ray source. The 35-day periodicity is also seen in the regular variations of the shape of the pulse profiles (Trümper et al. 1986; Staubert et al. 2013), which has also led to the suggestion that free precession of the neutron star may play a role (Trümper et al. 1986; Postnov et al. 2013), which is still an open question and highly debated. In the context of this work it is of interest whether the X-ray spectra show variations with phase of the 35-day modulation. This is indeed the case (Parmar et al. 1980; Mihara et al. 1991; Kuster et al. 2005; Vasco 2012). Staubert et al. 2014 had suggested that there is a weak modulation of the cyclotron line energy $E_{\rm cyc}$ during the *Main-On* and Vasco 2012 had found a strong variation of the power law index for 35-day phases greater than 0.16. The contribution of the series of *NuSTAR* observations of Her X-1, discussed here, is the following (for the limited range provided by the data used here, see Table 1): 1) The flux normalized $E_{\rm cyc}$ does not show any variation, the values are consistent with a constant. 2) The flux normalized values of $E_{\rm cut}$ and $E_{\rm fold}$ are constant up to the second highest 35-day phase observed (0.147 for Aug 2017, cycle 478), then both drop to significant lower values for the highest observed 35-day phase (0.202 for Feb. 2019, cycle 494). 3) The normalized power law index Γ behaves as the other two continuum parameters and drops to the lowest value (0.885) for the Feb. 2019 observation at 35-day phase 0.202.

4. Discussion

Correlations between spectral parameters were first discovered by comparing spectral parameters determined for different objects (Makishima & Mihara 1992; Makishima et al. 1999; Coburn et al. 2002). We now see, most prominently (but not only) in Her X-1, that strong correlations between spectral parameters, both continuum and line parameters, exist for individual objects, particularly related to changes in X-ray luminosity.

4.1. Correlation between line parameters

The linear correlation between the width of the cyclotron line and its centroid energy (Fig. 4) is expected from the fact that the line suffers a Doppler-broadening due to the thermal motion of the electron gas at a temperature kT_e. Applying the general formula for a Doppler-broadened line (of central energy E) to the resonant cyclotron scattering of photons on electrons, we write $\sigma = {\rm E}\,(kT_e/m_e\,c^2)^{1/2}$.[6] Since electrons in a strong magnetic field can move freely only in one dimension (along the field lines) we need to multiply by $cos\ \theta$, with θ being the the angle between the viewing direction and the magnetic field lines. The temperature of the electron gas is kT_e and the rest mass of the electron is $m_e\,c^2 \approx 511$ keV, so the electron temperature can be estimated to kT_e [keV] $\approx 511\ (\sigma/E_{\rm cyc})^2/|cos^2\Theta|$. The line broadening effect

[6] The general formula for a Doppler-broadened line is FWHM = E × (8 $ln2\ kT_e$ / $m_e\,c^2$)$^{1/2}$, with E being the line energy and FWHM = σ (8 $ln2$)$^{1/2}$ = 2.356 σ being the full width-at-half-maximum (see e.g., K.R. Lang, Astrophysical Formulae, Springer).

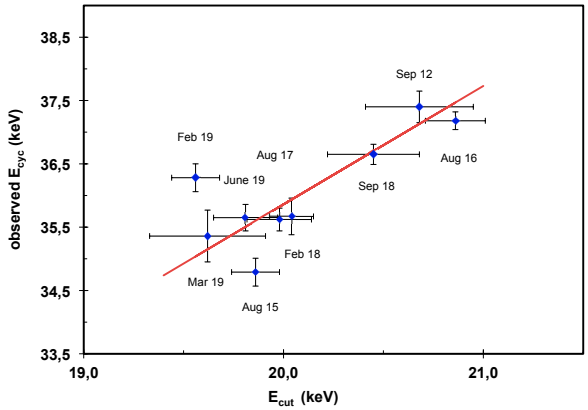

Fig. 11. The observed cyclotron line energy versus $E_{\rm cut}$. The best fit line is given by the function $E_{\rm cyc} = (35.86\pm0.11)+(1.87\pm0.36)\times(E_{\rm cut}-20.0)$ (all values in keV). Pearsons linear correlation coefficient is 0.79.

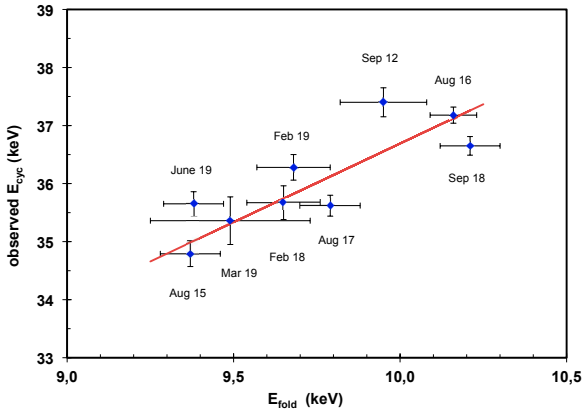

Fig. 12. The observed cyclotron line energy versus $E_{\rm fold}$. The best fit line is given by the function $E_{\rm cyc} = (36.69\pm0.13)+(2.71\pm0.39)\times(E_{\rm fold}-10.0)$ (all values in keV). Pearsons linear correlation coefficient is 0.82.

was already pointed out by Trümper et al. (1977) when the discovery of the first cyclotron line - in Her X-1 - was reported (see also Meszaros & Nagel 1985; Orlandini et al. 1998). It was then observationally confirmed when different cyclotron line energies and associated widths in several X-ray binaries were measured (Makishima et al. 1999; Coburn et al. 2002). Recently, it became possible to observe such correlations in individual sources, when the CRSF energy as well as the line width change with varying flux. Here we report the measurement for Her X-1: σ = 5.26 + 0.60 ($E_{\rm cyc}$ - 36.0) (all in keV). For small θ (cos $\theta \sim 1$), the calculated kT_e ranges from 8.3 keV to 13.5 keV, for flux values from 3 to 7 ASM-cts/s, respectively. This is very close to 10 keV which is the typical value of the continuum parameter $E_{\rm fold}$, often taken as the temperature of the plasma emitting the continuum. It is tempting to conclude that in Her X-1 we most likely see a pencil beam rather than a fan beam.

The fact that the relative line width $\sigma/E_{\rm cyc}$ increases with increasing flux (Fig. 5) means that the electron temperature kT_e increases with increasing flux. And so does $E_{\rm fold}$, as expected for an increasing accretion rate. However, the magnitude of the increase in kT_e is ∼12 % per unit flux, significantly stronger than the increase in $E_{\rm fold}$ with only ∼2 %. If $E_{\rm fold}$ is indeed a measure of the continuum temperature, then the electron temperature is increasing significantly faster.

The general dependence of σ on $E_{\rm cyc}$ for the known cyclotron line objects is demonstrated in Fig. 14 (up to $E_{\rm cyc}$ = 60 keV), where pairs of σ and $E_{\rm cyc}$ values are shown, taken from Coburn et al. (2002) and Staubert et al. (2019) (their Table A.5), together with a few individual objects. The central line through the rather scattered data defines a slope of ∼0.18 keV/keV, corresponding to a mean kT_e of ∼16 keV for Θ = 0. For a few objects we have now observed variations of both the line energy and the line width (physically introduced by a changing X-ray flux): Her X-1 (Staubert et al. 2007 and this work), GX 304−1 (Klochkov et al. 2015; Malacaria et al. 2015; Rothschild et al. 2017), Vela X-1 (La Parola et al. 2016) (the first harmonic) and Swift J1626.6−5156 (DeCesar et al. 2013) (see Fig. 14). For these few objects the absolute values of the relative widths are all rather small (they are all below the red line in Fig. 14, but the variation d(σ) / d($E_{\rm cyc}$), is significantly steeper (e.g., for Her X-1: 0.60 keV/keV), than for the complete ensemble.

We would like to stress that the X-ray flux (physically the mass accretion rate) is a fundamental parameter that seems to influence all spectral parameters. Apart from the line position and width, also its strength, its depth and its relative width are positively correlated with flux (see Table 3). The same is true for the continuum parameters $E_{\rm cut}$ and $E_{\rm fold}$ (Fig. 7 and Fig. 8), and - surprisingly (even if weak) - for the power law index Γ. We find that Γ increases with flux (by 1.8% for an increase in flux by a factor of two), while Klochkov et al. (2011), in pulse-amplitude-resolved spectroscopy of Her X-1, found the opposite trend (by 5.6%) - always in combination with an increase of $E_{\rm cyc}$ with flux. A solution may be given by Postnov et al. (2015) who showed (for several sources, but unfortunately not Her X-1) that the spectral hardness correlates with X-ray flux, consistent with Klochkov et al. (2011), but only up to a (source dependent) luminosity around a few times 10^{37} erg/s, after which the correlation stops, or even reverses. A luminosity of a few times 10^{37} erg/s is considered to be close to the border between the sub- and super-critical accretion regimes (Becker et al. 2012) at which the trend for these correlations reverses. Her X-1 is probably operating close to the critical luminosity, and the turning point for a reversal may actually be slightly different between the respective correlations.

An interesting correlation, first found by Coburn et al. (2002) among a group of X-ray binaries, namely the relative line width $\sigma_{\rm cyc}$ / $E_{\rm cyc}$ as function of the optical depth τ, is also realized in individual objects like 4U 1538−52 (Rodes-Roca et al. 2008) and in Her X-1 (Fig. 6). Coburn et al. (2002) and Rodes-Roca et al. (2008) note that simple theoretical models of cyclotron line generation actually predict the opposite dependence (Isenberg et al. 1998; Araya & Harding 1999).

Regarding inter-correlations between spectral parameters, it has been a general worry about how large the influence is of purely mathematical correlations introduced in the fitting process. Coburn et al. (2002) have tried to answer this question by performing Monte Carlo simulations, carefully designed for different types of correlations. Their conclusion was that formal correlations were not significant and that it was safe to conclude that the observed correlations are a true physical effect.

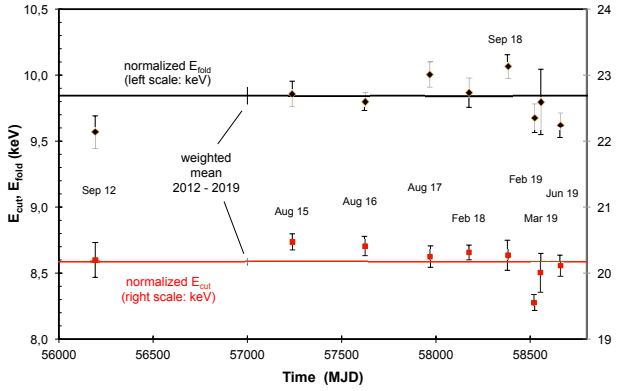

Fig. 13. Flux normalized values of $E_{\rm cut}$ (right scale) and $E_{\rm fold}$ (left scale) as function of time. The normalization is done to a reference X-ray flux of 5 (ASM-cts/s) using the linear correlations as stated in Table 3 and shown in Figs. 7 and 8. These two continuum parameters appear to be constant (see the horizontal l ines) over the time 2012–2019 (as the normalized cyclotron line energy $E_{\rm cyc}$, Fig. 2).

We have used the MCMC procedure offered in XSPEC to investigate the same question and present a corresponding analysis in Appendix A. We are confident that the observed correlations are indeed physical.

4.2. Physics behind changes of $E_{\rm cyc}$

The centroid energy of the cyclotron line in Her X-1 has been observed to change with respect to the following parameters (Staubert et al. 2014):
- pulse phase: 20% ((max-min)/mean) (Voges et al. 1982; Vasco et al. 2013; Staubert et al. 2014);
- X-ray flux: 6.5% for a change of flux by a factor of two (here and Staubert et al. 2007);
- elapsed time: constant around 35 keV from the discovery in 1975 to 1990, jump upward 1991–1994 from ∼35 keV to beyond 40 keV (∼20%) (Gruber et al. 2001; Staubert et al. 2007), followed by a well measured decay until ∼2012 down to ∼37 keV (10% over 16 years) (here and Staubert et al. 2014, 2016);
- and possibly a change by 1 keV or less with phase of the 35-day on-off-cycle (Staubert et al. 2014), which we do not confirm here.

The variation with pulse phase is believed to be due to the changing viewing angle under which the emission regions are seen (Schönherr et al. 2007). Vasco 2012[7] has shown that the above discussed correlation between the width and the centroid energy of the cyclotron line (and the dependence of both on flux) is also valid when certain pulse phases are analyzed (e.g., the line energy and the width are both at a maximum around the peak of the main pulse). We will not further discuss this phenomenon here, but concentrate on the dependence of the pulse phase averaged cyclotron line energy $E_{\rm cyc}$ on X-ray flux and on time.

4.2.1. Changes of $E_{\rm cyc}$ with flux

With respect to the physics at work behind the positive correlation of the pulse phase averaged cyclotron line energy with flux, we refer to discussions presented earlier by Staubert et al. (2007, 2014, 2016, 2017); Ji et al. (2019), as well as the theoretical work by Becker et al. (2012) (see also the summary and references given in the review by Staubert et al. (2019)). We repeat here only a few ideas. The dependence on luminosity (on both long and short timescales) could be due to a change in the height of the emission region above the neutron star surface. Within the concept of different "accretion regimes" (e.g., Becker et al. 2012), the negative $E_{\rm cyc}$ / $L_{\rm X}$ correlation in supercritical accretion ($L_{\rm X} \gtrsim 10^{37}$ erg s^{-1}, as in, e.g., V0332+53) is due to the movement of a radiation dominated shock (and the primary emission region) to larger distances from the neutron star surface (i.e., to a weaker B-field), when the accretion rate increases. The opposite is expected to happen at subcritical accretion rates. Staubert et al. (2007) have shown that a positive correlation is actually expected in the case of lower accretion rates. Under this condition, the dynamical pressure of the in-falling material reduces the height of the emission region when the accretion rate increases, leading to an increase in E_{cyc}, as was also found by Becker et al. (2012). Recently, a model involving a collisionless shock was developed that also explains the deviation from a pure linear dependence (a "roll-off"), as observed in GX 304−1 (Rothschild et al. 2017; Vybornov et al. 2017).

Alternatively, or in combination with a height-related effect, the observed variations could be due to changes of the configuration of the magnetic field when the accretion rate varies. As Mukherjee et al. (2013, 2014) have shown, the usually assumed dipole structure of the magnetic field is significantly altered when the mass accretion rate changes. Close to the magnetic poles, a higher accretion rate can lead to a significant increase of the density of field lines at the outer circumference of the accretion mound when the in-falling material pushes matter and field lines from the center radially outward (see also below).

4.2.2. Changes of $E_{\rm cyc}$ with time

The dependence of $E_{\rm cyc}$ on time is even less well understood. With regard to the long-term decay of $E_{\rm cyc}$, we think that it is either a geometric displacement of the emission region or a change in the local field configuration e.g., as calculated by Mukherjee & Bhattacharya (2012), rather than a change in the strength of the underlying global dipole. Staubert (2014) has suggested that the observed change of $E_{\rm cyc}$ may be connected to a slight imbalance between "gain" and "loss" of accreted material, such that the structure of the accretion mound changes with time. With an accretion rate of $\sim 10^{17}$ g/s a variation on relatively short time scales does not seem implausible. If the "gain" is slightly larger than the "loss", material would slowly accumulate in the mound, possibly increasing its height or changing the local field structure, which might be the reason for the long-term reduction in $E_{\rm cyc}$. One might expect, that this reduction can find a natural end (e.g., when the excess mass and the associated pressure in the accretion mound becomes too large), such that a forced outflow of material to larger areas of the NS surface causes a re-adjustment of the accretion mound back to the unperturbed configuration. This could be a relatively fast and catastrophic event – possibly explaining the rather sudden upward jump in $E_{\rm cyc}$ observed between 1990 and 1993. The time period 1990-2012 sets an apparent time scale of instability: a few years of very fast change – the increase in $E_{\rm cyc}$ by ∼5 keV –, followed by ∼16 years of decay down to the original level. A corresponding time scale for stability is not yet known. Future observations should search for indications for an increase or even a new upward jump in $E_{\rm cyc}$.

[7] PhD thesis by Davide Vasco, 2012, University of Tübingen, Germany, http://nbn-resolving.de/urn:nbn:de:bsz:21-opus-63466

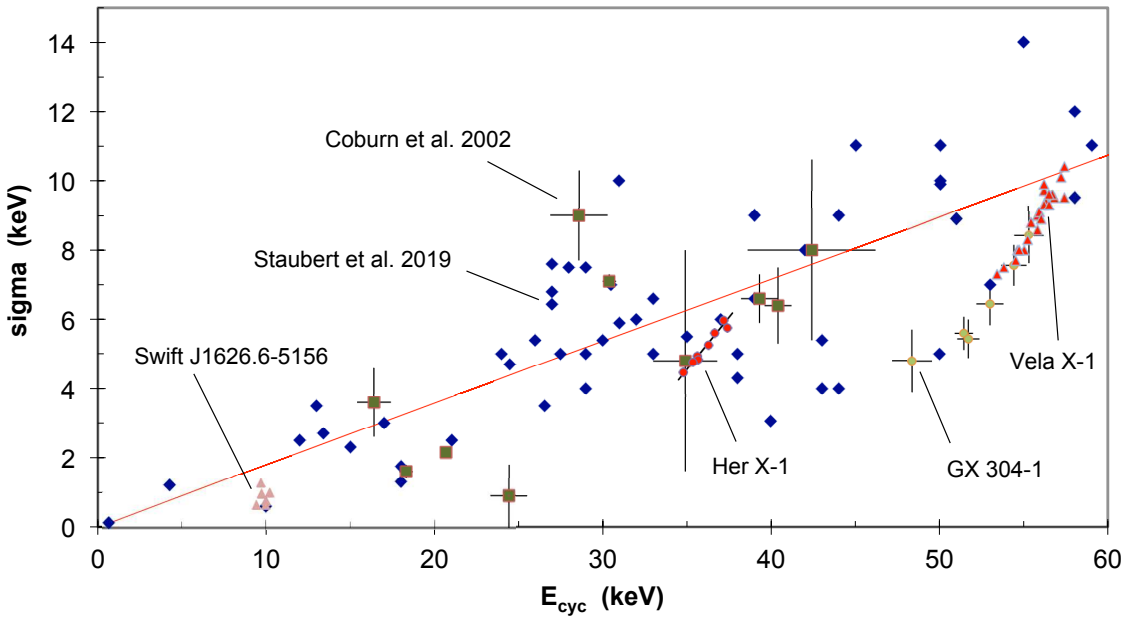

Fig. 14. Correlation between the width (sigma) and the centroid energy of cyclotron lines for different X-ray binaries. The blue rhombs are data from the compilation in Staubert et al. (2019), the filled squares (with uncertainties) are from Coburn et al. (2002). The red line is a fit to these two data sets defining $\sigma = 0.19\ E_{\rm cyc}$. The individual sources shown are: GX 304−1 (Klochkov et al. 2015), Swift J1626.6−5156 (DeCesar et al. 2013), Vela X-1 (La Parola et al. 2016) and Her X-1 (same as Fig. 4).

Since an upward movement could be rather fast (similar to the earlier event), it is important to observe as regularly as possible, in order not to miss such an event again.

5. Summary

Her X-1 has been well monitored during the last decade, mostly by *NuSTAR*, but also by *INTEGRAL* and *Swift*/BAT, and more recently by *Insight*-HXMT and *Astrosat*[8]. Her X-1 is actually the only highly magnetized accreting pulsar for which repeated observations over longer periods of time exist. This has provided the base for the discovery of new phenomena, like the dependence of the cyclotron line energy (as well as almost all spectral parameters) on flux and the long-term decay of the cyclotron line energy over nearly 20 years. Both of these phenomena have meanwhile been seen in other accreting X-ray binary pulsars (see the review by Staubert et al. 2019).

The results of nine *NuSTAR* observations of Her X-1 between 2012 and 2019 are the following:
- The dependence of the cyclotron line energy on X-ray flux, discovered in 2007, is confirmed and measured with high precision.
- The flux-normalized cyclotron line energy is constant since (at least) ~2012. The previously reported long-term decay has ended.
- All cyclotron line parameters - the line energy $E_{\rm cyc}$, the width σ, the strength, the optical depth τ and the relative width - show a positive and linear correlation to X-ray flux.
- The former statement also means that all cyclotron line parameters correlate positively and linearly with one-another.
- The continuum parameters $E_{\rm cut}$ and $E_{\rm fold}$ correlate positively and linearly with X-ray flux. The flux-normalized continuum parameters are consistent with constant values since 2012. The third continuum parameter, the power law index Γ, shows a weak positive correlation with flux. This is the opposite of what was seen before in a pulse-amplitude-resolved analysis, which may have a somewhat different meaning. The interpretation of the different observed correlations with regard to the prevailing accretion regimes (sub- or supercritical) is not so simple.
- We have learned that there are correlations between continuum parameters and line parameters.
- The correlations of the line and continuum parameters with X-ray flux and among each other are considered to reflect true physical correlations, which have yet to be investigated and explained by theoretical modeling. As shown in the Appendix, the analysis of the purely mathematical correlation between fitting parameters has led to the conclusion that those are not significant.

We urge that the source continues to be observed regularly. For 2020 this seems to be secured through already planned observations (partly simultaneous) between *INTEGRAL*, *NuSTAR*, *XMM-Newton* and *Insight*-HXMT. At the same time, it would be very important that theoretical models be developed further.

Acknowledgements. We would like to acknowledge the dedication of all the people who have contributed to the great success of all relevant missions, in particular *NuSTAR*. We especially thank the "schedulers", foremost Karl Forster, for

[8] Papers by Xiao et al. and Bala et al. are in preparation

his efforts with respect to the non-standard scheduling of the observations of Her X-1. We acknowledge the historical contributions to the subject at hand by Dmitry Klochkov.

References

Araya, R. & Harding, A. 1999, ApJ, 517, 334
Becker, P. A., Klochkov, D., Schönherr, G., et al. 2012, A&A, 544, A123
Caballero, I. & Wilms, J. 2012, Mem. Soc. Astron. Italiana, 83, 230
Coburn, W., Heindl, W. A., Rothschild, R. E., et al. 2002, ApJ, 580, 394
Cusumano, G., La Parola, V., D'Aì, A., et al. 2016, MNRAS, 460, L99
DeCesar, M. E., Boyd, P. T., Pottschmidt, K., et al. 2013, ApJ, 762, 61
Doroshenko, V., Tsygankov, S. S., Mushtukov, A. e. A., et al. 2017, MNRAS, 466, 2143
Foreman-Mackey, D., Hogg, D. W., Lang, D., & Goodman, J. 2013, PASP, 125, 306
Fürst, F., Grefenstette, B. W., Staubert, R., et al. 2013, ApJ, 779, 69
Gruber, D. E., Heindl, W. A., Rothschild, R. E., et al. 2001, ApJ, 562, 499
Harrison, F. A., Craig, W. W., Christensen, F. E., et al. 2013, ApJ, 770, 103
Heindl, W. A., Rothschild, R. E., Coburn, W., et al. 2004, in American Institute of Physics Conference Series, Vol. 714, X-ray Timing 2003: Rossi and Beyond, ed. P. Kaaret, F. K. Lamb, & J. H. Swank, 323–330
Hemphill, P. B., Rothschild, R. E., Fürst, F., et al. 2016, MNRAS, 458, 2745
Isenberg, M., Lamb, D. Q., & Wang, J. C. L. 1998, ApJ, 493, 154
Ji, L., Staubert, R., Ducci, L., et al. 2019, MNRAS, 484, 3797
Klochkov, D., Staubert, R., Postnov, K., et al. 2015, A&A, 578, A88
Klochkov, D., Staubert, R., Santangelo, A., Rothschild, R. E., & Ferrigno, C. 2011, A&A, 532, A126
Kuster, M., Wilms, J., Staubert, R., et al. 2005, A&A, 443, 753
La Parola, V., Cusumano, G., Segreto, A., & D'Aì, A. 2016, MNRAS, 463, 185
Makishima, K. & Mihara. 1992, Frontiers O X-ray Astronomy (Universal Academy Press Inc, Tokyo), 23
Makishima, K., Mihara, T., Nagase, F., & Tanaka, Y. 1999, ApJ, 525, 978
Malacaria, C., Klochkov, D., Santangelo, A., & Staubert, R. 2015, A&A, 581, A121
Meszaros, P. & Nagel, W. 1985, ApJ, 298, 147
Mihara, T., Ohashi, T., Makishima, K., et al. 1991, PASJ, 43, 501
Mukherjee, D. & Bhattacharya, D. 2012, MNRAS, 420, 720
Mukherjee, D., Bhattacharya, D., & Mignone, A. 2013, MNRAS, 435, 718
Mukherjee, D., Bhattacharya, D., & Mignone, A. 2014, in European Physical Journal Web of Conferences, Vol. 64, European Physical Journal Web of Conferences, 2004
Orlandini, M., Dal Fiume, D., Frontera, F., et al. 1998, ApJ, 500, L163
Parmar, A. N., Sanford, P. W., & Fabian, A. C. 1980, MNRAS, 192, 311
Petterson, J. A. 1977, ApJ, 218, 783
Postnov, K., Shakura, N., Staubert, R., et al. 2013, MNRAS, 435, 1147
Postnov, K. A., Gornostaev, M. I., Klochkov, D., et al. 2015, MNRAS, 452, 1601
Revnivtsev, M. & Mereghetti, S. 2016, Magnetic Fields of Neutron Stars in X-Ray Binaries, Vol. 54 (Springer 2016), 299
Rodes-Roca, J., Torrejón, J. M., & Bernabéu, J. G. 2008, The fundamental cyclotron line in 4U 1538-52, Vol. 3, 189–200
Rothschild, R. E., Kühnel, M., Pottschmidt, K., et al. 2017, MNRAS, 466, 2752
Schandl, S. & Meyer, F. 1994, A&A, 289, 149
Schönherr, G., Wilms, J., Kretschmar, P., et al. 2007, A&A, 472, 353
Schwarm, F.-W., Schönherr, G., Falkner, S., et al. 2017, A&A, 597, A3
Staubert, R. 2003, in Multifrequency behaviour of high energy cosmic sources, ed. L.S.-G.F. Giovanelli, Vol. ChJAA, Vol. 3, S270
Staubert, R. 2014, in PoS(INTEGRAL2014)024
Staubert, R., Bezler, M., & Kendziorra, E. 1983, A&A, 117, 215
Staubert, R., Klochkov, D., Fürst, F., et al. 2017, A&A, 606, L13
Staubert, R., Klochkov, D., Vasco, D., et al. 2013, A&A, 550, A110
Staubert, R., Klochkov, D., Vybornov, V., Wilms, J., & Harrison, F. A. 2016, A&A, 590, A91
Staubert, R., Klochkov, D., Wilms, J., et al. 2014, A&A, 572, A119
Staubert, R., Shakura, N. I., Postnov, K., et al. 2007, A&A, 465, L25
Staubert, R., Trümper, J., Kendziorra, E., et al. 2019, A&A, 622, A61
Tananbaum, H., Gursky, H., Kellogg, E. M., et al. 1972, ApJ, 174, L143
Terada, Y., Mihara, T., Nagase, F., et al. 2007, Adv. in Space Research, 40, 1485
Trümper, J., Kahabka, P., Oegelman, H., Pietsch, W., & Voges, W. 1986, ApJ, 300, L63
Trümper, J., Pietsch, W., Reppin, C., et al. 1978, ApJ, 219, L105
Trümper, J. et al. 1977, Ann. N.Y. Acad. Sci., 302, 538
Vasco, D. 2012, PhD thesis, Univ. of Tübingen
Vasco, D., Staubert, R., Klochkov, D., et al. 2013, A&A, 550, A111
Voges, W., Pietsch, W., Reppin, C., et al. 1982, ApJ, 263, 803
Vybornov, V., Doroshenko, V., Staubert, R., & Santangelo, A. 2018, A&A, 610, A88
Vybornov, V., Klochkov, D., Gornostaev, M., et al. 2017, A&A, 601, A126
Wilms, J. 2012, in Proceed. 39th COSPAR Sci. Assembly, 14-22 July 2012, Mysore, India, Vol. 39, 2159
Xiao, G. C., Ji, L., Staubert, R., et al. 2019, arXiv e-prints, arXiv:1910.02393

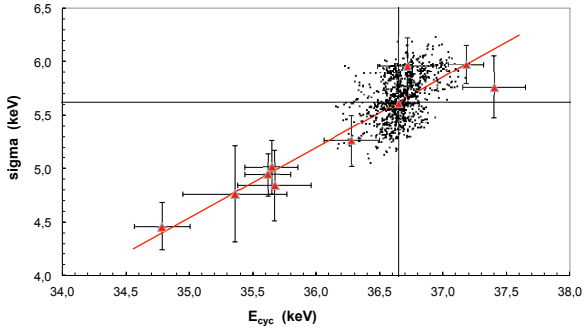

Fig. 15. The first 1000 sigma / $E_{\rm cyc}$ pairs of the MCMC simulation together with the measured correlation as shown in Fig. 4.

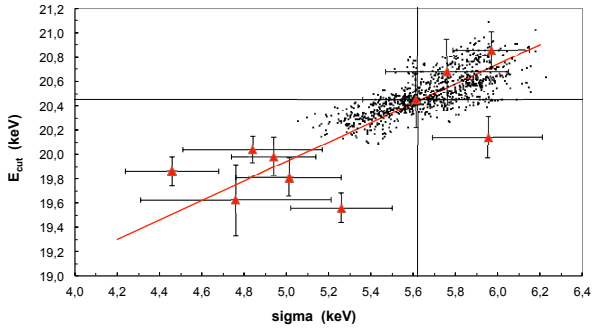

Fig. 16. The first 1000 $E_{\rm cut}$ / sigma pairs of the MCMC simulation together with the measured correlation.

6. Appendix

In the main text, we reported the correlations between spectral parameters observed from nine *NuSTAR* observations in 2012-2019. Here we ask how much model degeneracies during the spectral fitting contribute to theses correlations. We investigate this through Monte Carlo simulations. In practice, we adopted the best-fitting parameters of the *NuSTAR* observation in September 2018 as a reference model (with a flux of 5.6 (ASM-cts/s) this observation is close to the center of the flux range encountered between 2012 and 2019). With the statistics and the spectral parameters from this observation as an input model, we performed two different simulations (with 10^4 events each): first, a Markov Chain Monte Carlo (MCMC) simulation (provided by XSPEC[9]) which makes use of the Goodman-Weare algorithm[10] (see also Foreman-Mackey et al. (2013)), and second producing simulated spectra using the *fakeit* command in XSPEC with subsequently fitting these spectra. The two methods provided consistent results, we show the MCMC simulation in Fig. 17. As expected, most of the correlations between the parameters are weak, as is evident from the circular shape of the two-dimensional distributions. As an example we show the scatter plot of $\sigma_{\rm cyc}$ versus $E_{\rm cyc}$ of the first 1000 simulated

[9] https://heasarc.gsfc.nasa.gov/xanadu/xspec/
[10] https:///ui.adsabs.harvard.edu/abs/2010CAMCS...5...65G/abstract

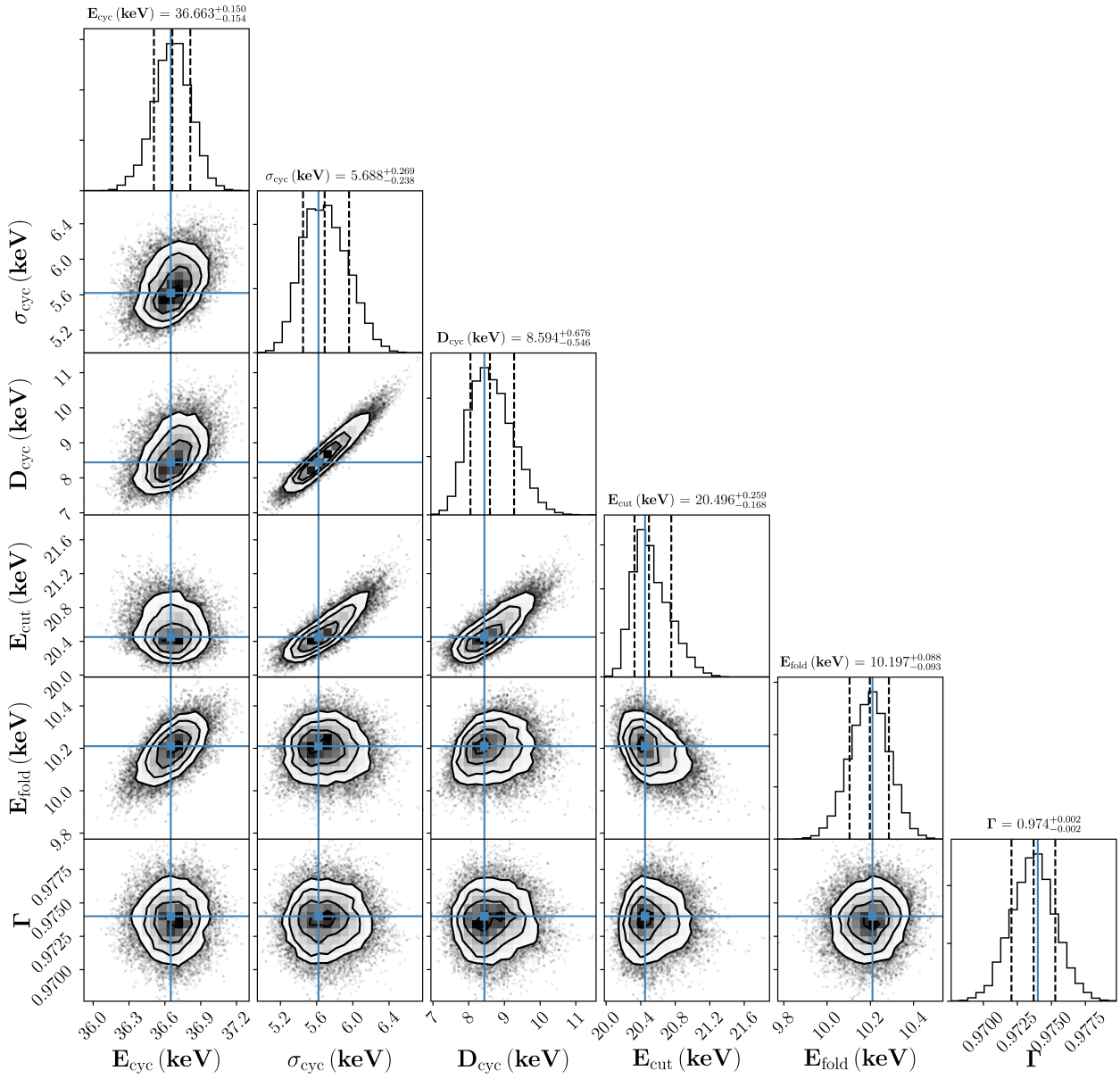

Fig. 17. The contours represent two-dimensional distributions of parameters obtained from Monte Carlo simulations at the significance level of 1, 2 and 3 σ, and the histograms are distributions for each variable. The blue lines are the input parameters used during the simulations.

MCMC spectra in Fig. 15. The range of observed $E_{\rm cyc}$ is a factor ~10 larger than the corresponding full width at half maximum (FWHM) of the simulated $E_{\rm cyc}$ distribution (for $\sigma_{\rm cyc}$ the factor is ~3.3). This shows that any model degeneracy has only a small contribution to the overall correlation. There are three distributions that are elongated (under roughly 45 degrees) indicating stronger correlations: $D_{\rm cyc}$[11] versus $\sigma_{\rm cyc}$, $E_{\rm cut}$ versus $\sigma_{\rm cyc}$ and $E_{\rm cut}$ versus $D_{\rm cyc}$. Even here the corresponding factors (FWHM / observed range) are between two and four. The correlation between $\sigma_{\rm cyc}$ and $D_{\rm cyc}$ is actually given through the definition: $D_{\rm cyc} = \sigma \times \tau \times \sqrt{2\pi}$. In Fig. 16 we show the degeneracy between the continuum parameter $E_{\rm cut}$ and the line parameter $\sigma_{\rm cyc}$. We conclude that the physical correlations discussed are real.

[11] $D_{\rm cyc}$ is called *strength* in the main text